Improved association in a classical density functional theory for water

Citation	Krebs, E. J., Schulte, J. B., & Roundy, D. (2014). Improved association in a classical density functional theory for water. Journal of Chemical Physics, 140(12), 124507. doi:10.1063/1.4869597
DOI	10.1063/1.4869597
Publisher	American Institute of Physics Publishing
Version	Version of Record
Citable Link	http://hdl.handle.net/1957/48225
Terms of Use	http://cdss.library.oregonstate.edu/sa-termsofuse

Improved association in a classical density functional theory for water

Eric J. Krebs, Jeff B. Schulte, and David Roundy
Department of Physics, Oregon State University, Corvallis, Oregon 97331, USA

(Received 5 September 2013; accepted 14 March 2014; published online 28 March 2014)

We present a modification to our recently published statistical associating fluid theory-based classical density functional theory for water. We have recently developed and tested a functional for the averaged radial distribution function at contact of the hard-sphere fluid that is dramatically more accurate at interfaces than earlier approximations. We now incorporate this improved functional into the association term of our free energy functional for water, improving its description of hydrogen bonding. We examine the effect of this improvement by studying two hard solutes (a hard hydrophobic rod and a hard sphere) and a Lennard-Jones approximation of a krypton atom solute. The improved functional leads to a moderate change in the density profile and a large decrease in the number of hydrogen bonds broken in the vicinity of the hard solutes. We find an improvement of the partial radial distribution for a krypton atom in water when compared with experiment. © *2014 AIP Publishing LLC*. [http://dx.doi.org/10.1063/1.4869597]

I. INTRODUCTION

Water, the universal solvent, is of critical practical importance, and a continuum description of water is in high demand for a solvation model. A number of recent attempts to develop improved solvation models for water have built on the approach of classical density functional theory (DFT).[1–7] Classical DFT is based on a description of a fluid written as a free energy functional of the density distribution. There are two general approaches used to construct a classical DFT for water. The first is to choose a convenient functional form which is then fit to properties of the bulk liquid at a given temperature and pressure.[1–8] Using this approach, it is possible to construct a functional that reproduces the exact second-order response function of the liquid under the fitted conditions. However, this class of functional will be less accurate at other temperatures or pressures—and in the inhomogeneous scenarios in which solvation models are applied. The second approach is to construct a functional by applying liquid-state theory to a model system, and then fit the model to experimental data such as the equation of state.[9–19]

A widely used family of models used in the development of classical density functionals is based on Statistical Associating Fluid Theory (SAFT).[20] SAFT is a theory based on a model of hard spheres with weak dispersion interactions and hydrogen-bonding association sites, which has been used to accurately model the equations of state of both pure fluids and mixtures over a wide range of temperatures and pressures.[21,22] The association contribution to the free energy uses Wertheim's first-order thermodynamic perturbation theory to describe an associating fluid as hard spheres with strong associative interactions at specific sites on the surface of each sphere.[23–26] These association sites have an attractive interaction at contact, and rely on the hard-sphere pair distribution function at contact g_σ^{HS} in order to determine the extent of association. While this function is known for the homogeneous hard-sphere fluid, it must be approximated for inhomogeneous systems, such as occur at liquid interfaces.

In a recent paper, we examined the pair distribution function at contact in various inhomogeneous configurations.[27] We tested the accuracy of existing approximations for the pair distribution function at contact,[28,29] and derived a significantly improved approximation for the averaged distribution function at contact. In this paper, we apply this improved g_σ^{HS} to the SAFT-based classical density functional for water developed by Hughes *et al.*[9] This functional was constructed to reduce in the homogeneous limit to the 4-site optimal SAFT model for water developed by Clark *et al.*[10] The DFT of Hughes *et al.*[9] uses the association free energy functional of Yu and Wu,[28] which is based on a g_σ^{HS} that we have since found to be inaccurate.[27] In this paper, we will examine the result of using the improved functional for g_σ^{HS} developed in Schulte *et al.*[27] to construct an association free energy functional.

II. METHOD

The classical density functional for water of Hughes *et al.*[9] consists of four terms

$$F[n(\mathbf{r})] = F_{\mathrm{ideal}}[n(\mathbf{r})] + F_{\mathrm{HS}}[n(\mathbf{r})] + F_{\mathrm{disp}}[n(\mathbf{r})] + F_{\mathrm{assoc}}[n(\mathbf{r})], \quad (1)$$

where F_{ideal} is the ideal gas free energy and F_{HS} is the hard-sphere excess free energy, for which we use the White Bear functional.[30] F_{disp} is the free energy contribution due to the square-well dispersion interaction; this term contains one empirical parameter, s_d, which is used to fit the surface tension of water near one atmosphere (see Fig. 1). Finally, F_{assoc} is the free energy contribution due to association, which is the term that we examine in this paper.

A. Dispersion

The dispersion term in the free energy includes the van der Waals attraction and any orientation-independent

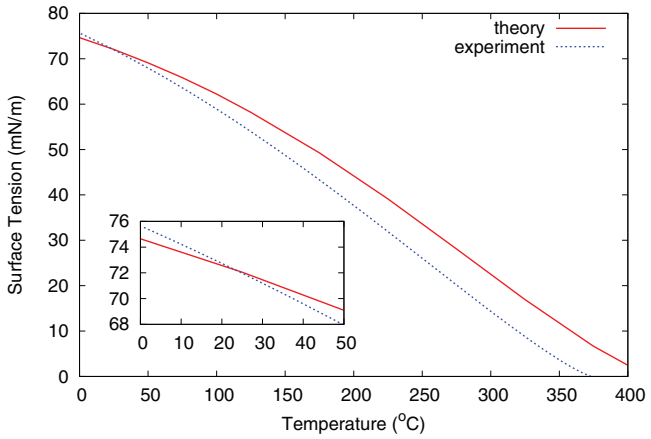

FIG. 1. Comparison of surface tension versus temperature for theoretical and experimental data. The experimental data are taken from NIST.[33] The length-scaling parameter s_d is fit so that the theoretical surface tension will match the experimental surface tension near room temperature.

interactions. Following Hughes *et al.*,[9] we use a dispersion term based on the SAFT-VR approach,[31] which has two free parameters (taken from Clark *et al.*[10]): an interaction energy ϵ_d and a length scale $\lambda_d R$.

The SAFT-VR dispersion free energy has the form[31]

$$F_{\text{disp}}[n] = \int \left(a_1(\mathbf{r}) + \beta a_2(\mathbf{r})\right) n(\mathbf{r}) d\mathbf{r}, \tag{2}$$

where a_1 and a_2 are the first two terms in a high-temperature perturbation expansion and $\beta = 1/k_B T$. The first term, a_1, is the mean-field dispersion interaction. The second term, a_2, describes the effect of fluctuations resulting from compression of the fluid due to the dispersion interaction itself, and is approximated using the local compressibility approximation (LCA), which assumes the energy fluctuation is simply related to the compressibility of a hard-sphere reference fluid.[32]

The form of a_1 and a_2 for SAFT-VR is given in Ref. 31, expressed in terms of the packing fraction. In order to apply this form to an *inhomogeneous* density distribution, we construct an effective local packing fraction for dispersion η_d, given by a Gaussian convolution of the density

$$\eta_d(\mathbf{r}) = \frac{1}{6\sqrt{\pi}\lambda_d^3 s_d^3} \int n(\mathbf{r}') \exp\left(-\frac{|\mathbf{r}-\mathbf{r}'|^2}{2(2\lambda_d s_d R)^2}\right) d\mathbf{r}'. \tag{3}$$

This effective packing fraction is used throughout the dispersion functional, and represents a packing fraction averaged over the effective range of the dispersive interaction. Equation (3) contains an additional empirical parameter s_d introduced by Hughes *et al.*,[9] which modifies the length scale over which the dispersion interaction is correlated.

B. Association

The association free energy for our four-site model has the form

$$F_{\text{assoc}}[n] = k_B T \int n_{\text{site}}(\mathbf{r}) \left(\ln X(\mathbf{r}) - \frac{X(\mathbf{r})}{2} + \frac{1}{2}\right) d\mathbf{r}, \tag{4}$$

where $n_{\text{site}}(\mathbf{r})$ is the density of bonding sites at position $\mathbf{r}$

$$n_{\text{site}}(\mathbf{r}) = \begin{cases} 4n(\mathbf{r}) & \text{this work} \\ 4n_0(\mathbf{r})\zeta(\mathbf{r}) & \text{Hughes } et\ al.[9] \end{cases}, \tag{5}$$

where the factor of four comes from the four hydrogen bond sites, the fundamental measure $n_0(\mathbf{r})$ is the average density contacting point $\mathbf{r}$, and $\zeta(\mathbf{r})$ is a dimensionless measure of the density inhomogeneity from Yu and Wu.[28] The functional $X(\mathbf{r})$ is the fraction of association sites *not* hydrogen-bonded, which is determined for our 4-site model by the quadratic equation

$$X(\mathbf{r}) = \frac{\sqrt{1 + 2n'_{\text{site}}(\mathbf{r})\kappa_a g_\sigma^{SW}(\mathbf{r})\left(e^{\beta\epsilon_a} - 1\right)} - 1}{n'_{\text{site}}(\mathbf{r})\kappa_a g_\sigma^{SW}(\mathbf{r})\left(e^{\beta\epsilon_a} - 1\right)}, \tag{6}$$

where

$$n'_{\text{site}}(\mathbf{r}) = \begin{cases} \frac{4}{\pi\sigma^2}\int n(\mathbf{r}')\delta(\sigma - |\mathbf{r}-\mathbf{r}'|)d\mathbf{r}' & \text{this work} \\ 4n_0(\mathbf{r})\zeta(\mathbf{r}) & \text{Hughes } et\ al.[9] \end{cases} \tag{7}$$

is the density of bonding sites that could bond to the sites $n_{\text{site}}(\mathbf{r})$, and

$$g_\sigma^{SW}(\mathbf{r}) = g_\sigma^{HS}(\mathbf{r}) + \frac{1}{4}\beta\left(\frac{\partial a_1}{\partial \eta_d(\mathbf{r})} - \frac{\lambda_d}{3\eta_d}\frac{\partial a_1}{\partial \lambda_d}\right), \tag{8}$$

where g_σ^{HS} is the correlation function evaluated at contact for a hard-sphere fluid with a square-well dispersion potential, and a_1 and a_2 are the two terms in the dispersion free energy defined below Eq. (2). The radial distribution function of the square-well fluid g_σ^{SW} is written as a perturbative correction to the hard-sphere radial distribution function g_σ^{HS}. The functional of Hughes *et al.*[9] uses the g_σ^{HS} from Yu and Wu.[28] In this work, we use the g_σ^{HS} derived by Schulte *et al.*[27]

As in Hughes *et al.*,[9] we use Clark's five empirical parameters, and fit the calculated surface tension to experimental surface tension at ambient conditions by tuning the parameter s_d, which adjusts the length-scale of the average density used for the dispersion interaction. With the improved association term, we find these agree when s_d is 0.454, which is an increase from the value of 0.353 found by Hughes *et al.*[9] In order to explore further the change made by the improved association term, we compared the new functional with that of Hughes *et al.*[9] for the two hydrophobic cases of the hard rod and the hard spherical solute.

III. RESULTS

We will first discuss the case of a single hard rod immersed in water. Figure 2 shows the density profile of water near a rod with radius 1 Å. We have chosen to focus on this very small rod, which features a high density at contact and large density oscillations. As it must, the contact density drops as the radius of the rod increases, and the density profile approaches the smooth density profile of the liquid-vapor interface. The density computed using the functional of this paper is qualitatively similar to that from Hughes *et al.*,[9] with a

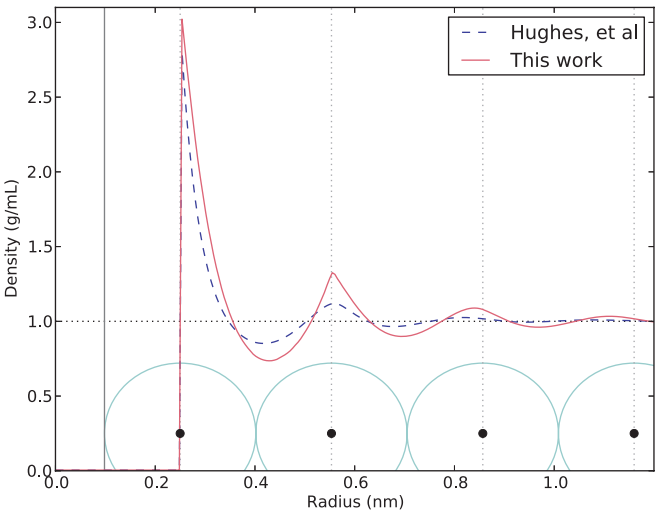

FIG. 2. Density profiles for a water around a single hard rod of radius 0.1 nm. The solid red profile is from the functional developed in this paper and the dashed blue profile is the result from Hughes *et al.*[9] For scale, under the profiles is a cartoon of a string of hard spheres touching in one dimension. The horizontal black dotted line is the bulk density for water and the vertical line on the left at 0.1 nm represents the rod wall.

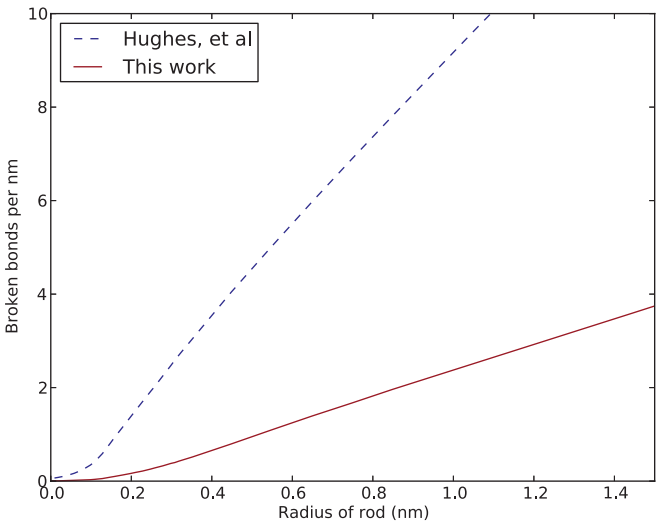

FIG. 3. Broken hydrogen bonds per nanometer for hard rods immersed in water. The solid red line uses the functional developed in this paper while the dashed blue line uses the functional from Hughes *et al.*[9] For large enough rods, the graph increases linearly for both functionals.

comparable density at contact—consistent with having made only a moderate change in the free energy. The first density peak near the surface is higher than that from Hughes *et al.*,[9] and the peak has a kink at the top. This reflects the improved accuracy of the g_σ^{HS} from Hughes *et al.*,[9] since beyond the first peak water molecules are unable to touch—or hydrogen bond to—molecules at the surface of the hard rod. This is illustrated under the profiles in Figure 2 by a cartoon of adjacent hard spheres that are increasingly distant from the hard rod surface.

In addition to the density, we examine the number of hydrogen bonds which are broken due to the presence of a hard rod. We define this quantity as

$$N_{\text{broken HB}} = 2\int (X(\mathbf{r}) - X_{\text{bulk}}) n_{\text{site}}(\mathbf{r}) d\mathbf{r}, \tag{9}$$

where $X_{\text{bulk}} = 0.13$ is the fraction of unbonded association sites in the bulk. The factor of 2 is chosen to account for the four association sites per molecule, and the fact that each broken hydrogen bond must be represented twice—once for each of the molecules involved. In Fig. 3, we show the number of hydrogen bonds broken by a hard rod per nanometer length, as predicted by the functional of Hughes *et al.*[9] (dashed line) and this work (solid line), as a function of the radius of the hard rod. In each case in the limit of large rods, the number of broken bonds is proportional to the surface area. At every radius, the functional of Hughes *et al.*[9] predicts approximately four times as many broken hydrogen bonds as the improved functional.

A common test case for studying hydrophobic solutes in water is the hard-sphere solute. Figure 4 shows results for the number of broken hydrogen bonds caused by a hard-sphere solute, as a function of the solute radius. As in Fig. 3, the number of broken bonds scales with surface area for large solutes, and the number of broken bonds is about four times smaller than the number from the functional of Hughes *et al.*[9]

For solutes smaller than 3 Å in radius, there is less than a tenth of a hydrogen bond broken. This is consistent with the well-known fact that small solutes (unlike large solutes) do not disrupt the hydrogen-bonding network of water.[34]

Finally, in order to compare with experimental results, we examined the hydration of Krypton. To describe the interaction of water with krypton, we use a Lennard-Jones potential with values $\epsilon = 0.9518$ kJ/mol and $\sigma = 3.42$ Å calculated using the Lorentz-Berthelot mixing rules and the Lennard-Jones parameters for water from SPC/E calculations.[35] Figure 5 shows the krypton-oxygen partial radial distribution function $g_{\text{Kr-O}}(r)$, which gives the relative probability density that an oxygen atom resides at a distance r from a krypton atom centered at the origin. We present theoretical curves computed using both this work and the functional of

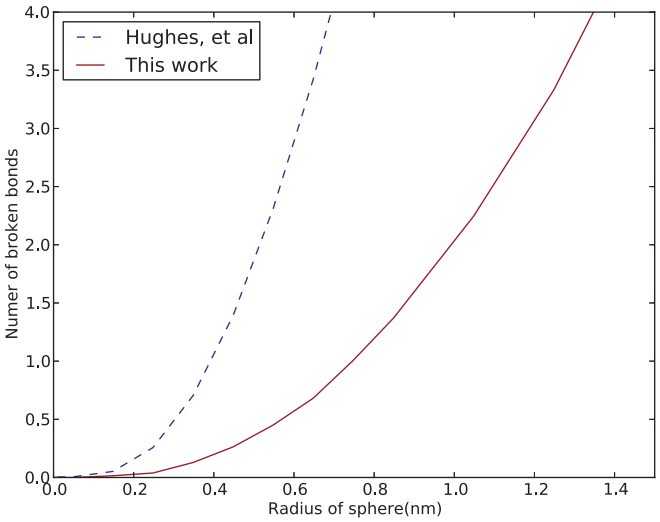

FIG. 4. Broken hydrogen bonds for hard spheres immersed in water. The solid red line uses our functional developed in this paper while the dashed blue line is from Hughes *et al.*[9]

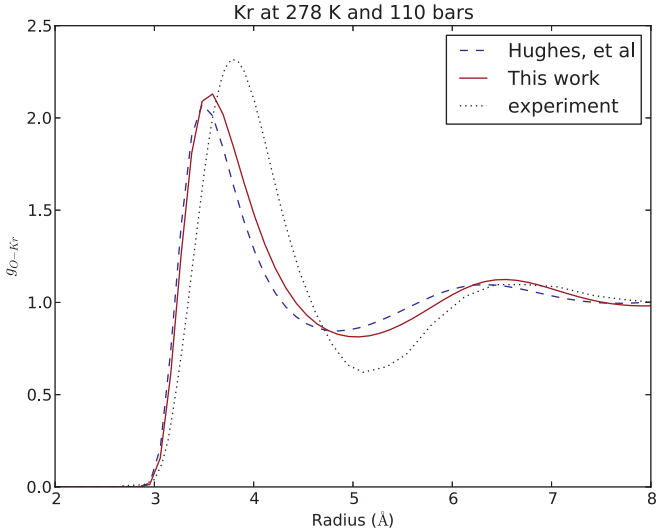

FIG. 5. The Kr–O partial radial distribution function at low temperature (5 °C) and high pressure (110 bars) in the limit of low concentration of krypton in water. The dashed blue line is computed using the functional from Hughes *et al.*,[9] the solid red line is this work, and the black dotted line is from experiment.[36]

Hughes *et al.*,[9] which we compare with experimental data from extended x-ray absorption fine structure spectroscopy (EXAFS).[36] The new functional shows improved agreement with experiment in the height and position of the first maximum as well as the height and position of the first minimum in $g_{\mathrm{Kr-O}}(r)$ when compared with that of Hughes *et al.*[9]

IV. CONCLUSION

We have modified the classical DFT for water developed by Hughes *et al.*[9] with the more accurate radial distribution function at contact developed by Schulte *et al.*,[27] which affects the predicted hydrogen bonding between water molecules. We found that while this modification has a relatively mild effect on the free energy and density profiles, it predicts fewer broken hydrogen bonds around hard hydrophobic solutes and at aqueous interfaces. The improved functional does indeed show better agreement with experiment when used to compute the partial radial distribution function of a krypton atom dissolved in water.

[1]G. Jeanmairet, M. Levesque, R. Vuilleumier, and D. Borgis, J. Phys. Chem. Lett. **4**, 619 (2013).
[2]S. Zhao, R. Ramirez, R. Vuilleumier, and D. Borgis, J. Chem. Phys. **134**, 194102 (2011).
[3]S. Zhao, Z. Jin, and J. Wu, J. Phys. Chem. B **115**, 6971 (2011).
[4]R. Ramirez, M. Mareschal, and D. Borgis, Chem. Phys. **319**, 261 (2005).
[5]R. Ramirez and D. Borgis, J. Phys. Chem. B **109**, 6754 (2005).
[6]M. Levesque, V. Marry, B. Rotenberg, G. Jeanmairet, R. Vuilleumier, and D. Borgis, J. Chem. Phys. **137**, 224107 (2012).
[7]M. Levesque, R. Vuilleumier, and D. Borgis, J. Chem. Phys. **137**, 034115 (2012).
[8]J. Lischner and T. Arias, J. Phys. Chem. B **114**, 1946 (2010).
[9]J. Hughes, E. J. Krebs, and D. Roundy, J. Chem. Phys. **138**, 024509 (2013).
[10]G. Clark, A. Haslam, A. Galindo, and G. Jackson, Mol. Phys. **104**, 3561 (2006).
[11]G. Gloor, F. Blas, E. del Rio, E. de Miguel, and G. Jackson, Fluid Phase Equilib. **194–197**, 521 (2002).
[12]G. Gloor, G. Jackson, F. Blas, E. Del Río, and E. de Miguel, J. Chem. Phys. **121**, 12740 (2004).
[13]G. Gloor, G. Jackson, F. Blas, E. del Río, and E. de Miguel, J. Phys. Chem. C **111**, 15513 (2007).
[14]K. Jaqaman, K. Tuncay, and P. J. Ortoleva, J. Chem. Phys. **120**, 926 (2004).
[15]G. N. Chuev and V. F. Sokolov, J. Phys. Chem. B **110**, 18496 (2006).
[16]D. Fu and J. Wu, Ind. Eng. Chem. Res. **44**, 1120 (2005).
[17]S. Kiselev and J. Ely, Chem. Eng. Sci. **61**, 5107 (2006).
[18]F. Blas, E. Del Río, E. De Miguel, and G. Jackson, Mol. Phys. **99**, 1851 (2001).
[19]R. Sundararaman, K. Letchworth-Weaver, and T. A. Arias, J. Chem. Phys. **137**, 044107 (2012).
[20]W. Chapman, K. Gubbins, G. Jackson, and M. Radosz, Fluid Phase Equilib. **52**, 31 (1989).
[21]E. A. Müller and K. E. Gubbins, Ind. Eng. Chem. Res. **40**, 2193 (2001).
[22]S. P. Tan, H. Adidharma, and M. Radosz, Ind. Eng. Chem. Res. **47**, 8063 (2008).
[23]M. S. Wertheim, J. Stat. Phys. **35**, 19 (1984).
[24]M. S. Wertheim, J. Stat. Phys. **35**, 35 (1984).
[25]M. S. Wertheim, J. Stat. Phys. **42**, 459 (1986).
[26]M. S. Wertheim, J. Stat. Phys. **42**, 477 (1986).
[27]J. B. Schulte, P. A. Kreitzberg, C. V. Haglund, and D. Roundy, Phys. Rev. E **86**, 061201 (2012).
[28]Y. X. Yu and J. Wu, J. Chem. Phys. **116**, 7094 (2002).
[29]J. Gross, J. Chem. Phys. **131**, 204705 (2009).
[30]R. Roth, R. Evans, A. Lang, and G. Kahl, J. Phys.: Condens. Matter **14**, 12063 (2002).
[31]A. Gil-Villegas, A. Galindo, P. Whitehead, S. Mills, G. Jackson, and A. Burgess, J. Chem. Phys. **106**, 4168 (1997).
[32]J. Barker and D. Henderson, Rev. Mod. Phys. **48**, 587 (1976).
[33]E. W. Lemmon, M. O. McLinden, and D. G. Friend, "Thermophysical properties of fluid systems," *NIST Chemistry Webbook*, NIST Standard Reference Database No. 69 (National Institute of Standards and Technology, Gaithersburg, MD, 2010), see http://webbook.nist.gov (retrieved December 15, 2010).
[34]D. Chandler, Nature (London) **437**, 640 (2005).
[35]D. Paschek, J. Chem. Phys. **120**, 6674 (2004).
[36]D. T. Bowron, A. Filipponi, M. A. Roberts, and J. L. Finney, Phys. Rev. Lett. **81**, 4164 (1998).